Eur Radiol (2015) 25:3175–3186
DOI 10.1007/s00330-015-3757-5

MAGNETIC RESONANCE

Contrast enhancement of intracranial lesions at 1.5 T: comparison among 2D spin echo, black-blood (BB) Cube, and BB Cube-FLAIR sequences

SungWoon Im[1] · Ryuichiro Ashikaga[1] · Yukinobu Yagyu[1] · Tetsuya Wakayama[2] · Mitsuharu Miyoshi[2] · Tomoko Hyodo[1] · Izumi Imaoka[1] · Seishi Kumano[1] · Kazunari Ishii[1] · Takamichi Murakami[1]

Received: 22 June 2014 / Revised: 2 March 2015 / Accepted: 31 March 2015 / Published online: 1 May 2015

Abstract
Objectives The purpose of this study was to investigate the usefulness of T1W black-blood Cube (BB Cube) and T1W BB Cube fluid-attenuated inversion recovery (BB Cube-FLAIR) sequences for contrast-enhanced brain imaging, by evaluating flow-related artefacts, detectability, and contrast ratio (CR) of intracranial lesions among these sequences and T1W-SE.
Methods Phantom studies were performed to determine the optimal parameters of BB Cube and BB Cube-FLAIR. A clinical study in 23 patients with intracranial lesions was performed to evaluate the usefulness of these two sequences for the diagnosis of intracranial lesions compared with the conventional 2D T1W-SE sequence.
Results The phantom study revealed that the optimal parameters for contrast-enhanced T1W imaging were TR/TE=500 ms/minimum in BB Cube and TR/TE/TI=600 ms/minimum/300 ms in BB Cube-FLAIR imaging. In the clinical study, the degree of flow-related artefacts was significantly lower in BB Cube and BB Cube-FLAIR than in T1W-SE. Regarding tumour detection, BB Cube showed the best detectability; however, there were no significant differences in CR among the sequences.
Conclusions At 1.5 T, contrast-enhanced BB Cube was a better imaging sequence for detecting brain lesions than T1W-SE or BB Cube-FLAIR.

✉ SungWoon Im
im@radiol.med.kindai.ac.jp

[1] Department of Radiology, Kinki University Faculty of Medicine, 377-2 Ohno-Higashi, Osaka-Sayama, Osaka 589-8511, Japan

[2] MR Applications and Workflow, Asia Pacific, GE Healthcare Japan, 4-7-127, Asahigaoka, Hino 191-8503, Tokyo, Japan

Key Points
- *Cube is a single-slab 3D FSE imaging sequence.*
- *We applied a black-blood (BB) imaging technique to T1W Cube.*
- *At 1.5 T, contrast-enhanced T1W BB Cube was valuable for detecting brain lesions.*

Keywords Cube · 3D fast spin-echo (FSE) · black-blood (BB) imaging · Contrast enhancement · Magnetic resonance imaging

Introduction

The contrast enhancement effect of intracranial lesions is reported to be superior in two-dimensional (2D) T1-weighted spin-echo (T1W-SE) sequences compared with 2D or 3D gradient-echo (GRE) sequences at 1.5 T MRI, even when 3D GRE has thinner slice thickness and less partial volume effect [1, 2]. Therefore, 2D T1W-SE is widely used for screening neoplastic lesions. However, it takes a considerable length time to cover the whole brain with thin slices, and obstructive flow-related artefacts are sometimes seen, especially in the posterior cranial fossa, making it difficult to detect contrast-enhanced lesions. Recently, optimized forms of 3D fast spin-echo (FSE) imaging, including Cube, have become available. These can be used for a broad range of clinical applications [3].

In addition, some preparation techniques, such as spatial pre-saturation, double inversion recovery, and motion-sensitizing magnetization preparation, can be applied for black-blood (BB) imaging [4]. By applying a BB preparation technique to a 3D FSE sequence, T1W BB Cube can be expected to provide whole-brain images with thin slices and without flow-related artefacts. However, to our knowledge,

Table 1 Imaging parameters for the first phantom study (numbers in parentheses indicate the actual value of TE)

	2D SE	BB cube	BB Cube-FLAIR	BB Cube-FLAIR	BB Cube-FLAIR
FOV (cm)	30×30	30×21	30×21	30×21	30×21
Matrix size	320×320	256×256	256×256	256×256	256×256
TR (ms)	500	500	2000	1500	1000
TE (ms)	13	Minimum (17.1)	Minimum (18.3)	Minimum (18.3)	Minimum (18.3)
TI (ms)	-	-	714	518	307
Flip angle (degrees)	90	Variable	Variable	Variable	Variable
Slice thickness (mm)	6	2	2	2	2
NEX	0.75	1	1	1	1

there are no reports regarding gadolinium-enhanced BB Cube and BB Cube fluid-attenuated inversion recovery (FLAIR) imaging for brain lesion detection. The purpose of this study is to establish optimal acquisition parameters of BB Cube and BB Cube-FLAIR sequences for contrast-enhanced brain imaging at 1.5 T, and to compare flow-related artefacts and the detectability and contrast ratio (CR) of intracranial lesions among these pulse sequences and T1W-SE.

Materials and methods

MR imaging

All studies were performed on a 1.5 T clinical MRI system using a 12-channel phased-array head coil (Signa HDxt with head-neck-spine [HNS] coil; GE Healthcare, Milwaukee, WI, USA). Three T1W sequences—2D SE, BB Cube, and BB Cube-FLAIR—were used in this study. To achieve black-blood conditions, the motion-sensitized preparation technique was used with a velocity encoding gradient of 5 cm/s for 3 axes. Detailed acquisition parameters are provided in Tables 1, 2, 3, and 4 for the phantom and clinical studies. The echo time (TE) of the Cube sequences was changed depending on the other scan parameters, including field of view (FOV), readout matrix, bandwidth, and the angle of the prescribed imaging plane; however, the change in TE was under T1W imaging conditions.

Phantom study

The phantom study was conducted in two sessions in order to compare the contrast properties of T1W-SE, BB Cube, and BB Cube-FLAIR at room temperature (22.6 °C). In this study, the acquisition parameters of BB Cube were optimized to show the contrast most similar to that of T1W-SE, while those of BB Cube-FLAIR were optimized to show the best contrast between white matter and saline phantom with a T1 value similar to that of lesions.

In the first session, MR images acquired from bottle phantoms consisting of gadopentetate dimeglumine (Gd-DTPA) (Magnevist; Bayer Schering Pharma, Berlin, Germany) diluted with saline at Gd-DTPA concentrations of 0.01 to 3 mmol/L, corresponding to T1 values of 60 to 3000 ms, were obtained. The imaging parameters for T1W-SE, BB Cube, and BB Cube-FLAIR are shown in Table 1.

In the second session, sample tube phantoms diluted with saline at Gd-DTPA concentrations of 0.1, 0.5, 1.0, 5.0, and 10.0 mmol/L were placed surrounding the head and examined using the parameters shown in Table 2. Signal intensities (SI)

Table 2 Imaging parameters for the second phantom study (numbers in parentheses indicate the actual value of TE)

	2D SE	BB cube	BB Cube-FLAIR	BB Cube-FLAIR	BB Cube-FLAIR
FOV (cm)	22×22	22×22	22×22	22×22	22×22
Matrix size	320×320	224×224	224×224	224×224	224×224
TR (ms)	500	500	800	700	600
TE (ms)	13	minimum (17.8)	minimum (17.9)	minimum (17.9)	minimum (17.9)
TI (ms)	-	-	400	350	300
Flip angle (degrees)	90	variable	variable	variable	variable
Slice thickness (mm)	6	2	2	2	2
NEX	1	1	1	1	1

Table 3 Imaging parameters of pre-contrast MRI for the clinical study

	Sag. T2WI	Ax. DWI	Ax. T2W-FSE	Ax. T1W-SE
FOV (cm)	22×22	26×30	22×22	22×22
Matrix size	256×320	128×160	288×320	320×320
TR (ms)	4000	2500	4000	500
TE (ms)	82.1	82.1	104.4	13
TI (ms)	-	-	-	-
Flip angle (degrees)	90	90	90	90
Slice thickness (mm)	5	6	6	6
NEX	1	1	1	1
Scan time (min:sec)	1:09	1:00	2:32	2:26

in the sample tubes and normal white matter on the acquired 2D SE, BB Cube, and BB Cube-FLAIR images were compared. We calculated CR using the following equation: CR=(SI of sample tube – SI of white matter) / SI of white matter, where SI of the sample tube is the mean SI of the sample tube, and the SI of white matter is the mean SI of normal white matter.

Clinical study

This study was approved by the institutional review board of our hospital. From June 2012 to December 2012, 44 consecutive subjects with suspicion of brain lesion were enrolled (age range 30–85 years, average 65.2 years; male=22, female=22). Written informed consent was obtained from all participants after sufficient explanation of the study. Before the administration of Gd-DTPA (0.2 mL/Kg), sagittal T2W-FSE, axial diffusion-weighted images (DWI), axial T2W-FSE, and axial T1W-SE images were acquired, followed by coronal Cube-FLAIR. After the administration of Gd-DTPA, coronal T1W-SE, axial T1W-SE, BB Cube, and BB Cube-FLAIR were acquired. Detailed sequence parameters are provided in Tables 3 and 4.

In the actual procedure, T1W-SE, BB Cube, and BB Cube-FLAIR were started approximately 4 min after intravenous injection of Gd-DTPA contrast agent and finished 13 min after this injection. Studies have reported that there is no significant change between 3.5 min and 25 min after Gd-DTPA injection in the contrast-to-noise ratio (CNR) between grey matter and tumours with blood-brain barrier damage [5, 6]. Furthermore, to reduce the bias in time after contrast injection, we alternated the order of the pulse sequences every month: T1W-SE, BB Cube, and BB Cube-FLAIR to 22 subjects and T1W-SE, BB Cube-FLAIR, and BB Cube to the remaining 22 subjects. In consideration of the possibility of interruption of the MR examination, T1W-SE was performed first in these sequences.

Image analysis

Axial images of T1W-SE, BB Cube, and BB Cube-FLAIR were compared in terms of 1) the degree of intracranial flow-related artefacts, 2) detectability of intracranial enhanced lesions, and 3) the CR of intracranial enhanced lesions. Two well-trained radiologists evaluated images of the three sequences with regard to these three points in a blinded fashion. In the case of a discrepancy between the radiologists,

Table 4 Imaging parameters of post-contrast MRI for the clinical study (derived from the phantom study data) (numbers in parentheses indicate the actual value of TE)

	Cor. T1W-SE	Ax. T1W-SE	Ax. BB Cube	Ax. BB Cube-FLAIR
FOV (cm)	22×22	22×22	22×22	22×22
Matrix size	256×320	320×320	224×224	224×224
TR (ms)	580	500	500	600
TE (ms)	13	13	minimum (17.5-18.7)	minimum (17.64-18.15)
TI (ms)	-	-	-	300
Flip angle (degrees)	90	90	variable	variable
Slice thickness (mm)	6	6	2	2
NEX	1	1	1	1
Scan time (min:sec)	3:40	2:20	2:35	3:06

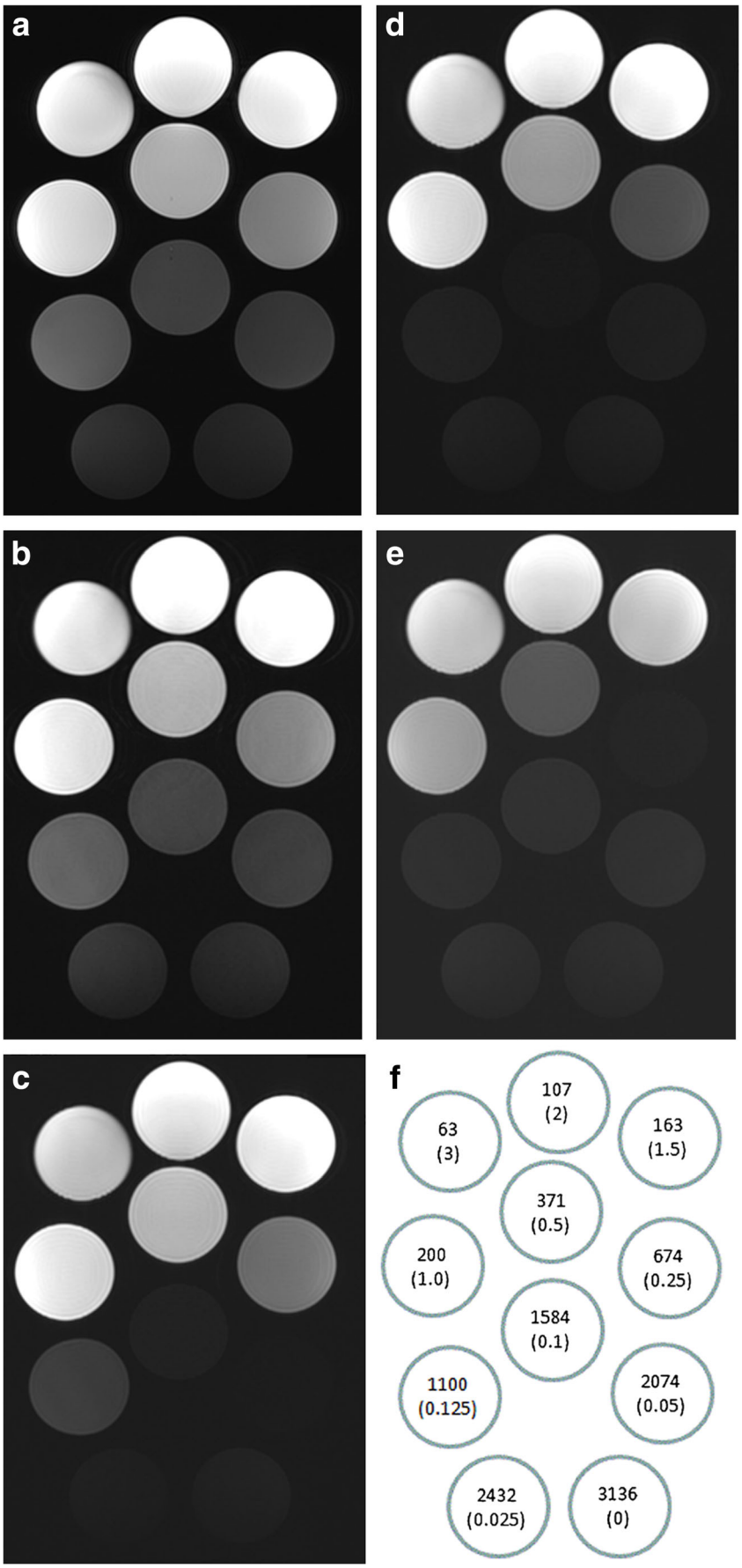
a
d
b
e
c
f
107
(2)
63
(3)
163
(1.5)
371
(0.5)
200
(1.0)
674
(0.25)
1584
(0.1)
1100
(0.125)
2074
(0.05)
2432
(0.025)
3136
(0)

◀ **Fig. 1** Images of bottle phantoms, (*a*) T1W-SE, (*b*) BB Cube, and (*c*-*e*) BB Cube-FLAIR, and (*f*) T1 values and Gd-DTPA concentrations of the phantoms. Numbers in parentheses show the Gd-DTPA concentration. BB Cube showed contrast very similar to that of T1W-SE. On the other hand, the contrast shown with BB Cube-FLAIR was different from that with T1W-SE and BB Cube

consensus was reached through subsequent discussion. The degree of flow-related artefacts in images of the 44 patients was scored by visualization of intracranial structures as follows: 0 (clearly visualized), 1 (some part of the structure was obscured), 2 (some part of the structure was visualized), or 3 (not visualized). The scores of the three sequences were compared using the Steel-Dwass test.

Regarding detectability of the lesions, each lesion was counted, measured, and classified according to its largest measured dimension in any imaging plane as either 5 mm and greater or less than 5 mm. The existence of contrast-enhanced lesions was determined by axial T1W-SE, BB Cube, and BB Cube-FLAIR in addition to coronal T1W-SE. Because surgical confirmation was not available in some of the subjects, the existence of contrast-enhanced lesions was considered true-positive if the enhanced lesions were observed in two different sequences or in two planes. Furthermore, we referred to clinical records and previous and/or follow-up MR or CT examination results. MR or CT examination results were obtained in all patients with enhanced brain lesions. The criterion standard of the number of intracranial enhanced lesions was determined by consensus between the two radiologists.

Detectability of the lesions among the three sequences was tested with Cochran's Q test, followed by multiple comparisons using the binomial test with Bonferroni adjustment; *p*-values of less than 0.05 were considered to indicate statistical significance. Differences between the number of enhanced lesions detected by each reader for each sequence and the criterion standard number of enhanced lesions were calculated. Additionally, differences between the number of enhanced lesions detected by the reader for each sequence at a 6-month interval and the criterion standard number of enhanced lesions were calculated. The kappa coefficient was used to assess the degree of interobserver and intraobserver agreements. Interpretation of the kappa coefficient was carried out according to the method proposed by Ladis and Kock [7].

With regard to CR measurement, the CR of 37 lesions in 18 subjects detected on all T1W-SE, BB Cube, and BB Cube-FLAIR were measured. Lesions with an area under 12.01 mm^2 or ring-enhanced thin-wall lesions were excluded

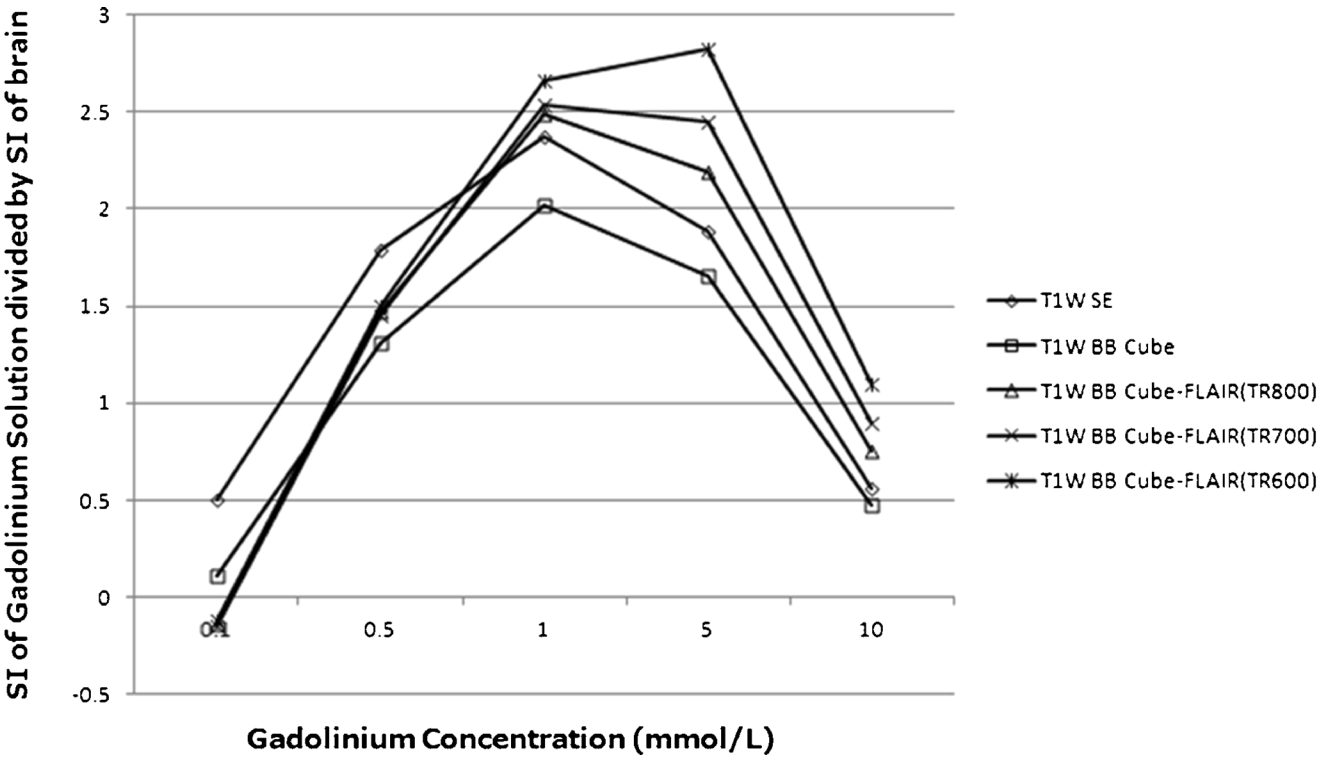

Fig. 2 Graph showing contrast enhancement ratios (CR) with different concentrations of Gd-DTPA on five pulse sequences. The vertical axis shows CR: CR=(SI of sample tube – SI of white matter) / SI of white matter. This result suggests that BB Cube-FLAIR shows better CR than T1W-SE or BB Cube at high Gd concentrations. In addition, the reduction of TR in BB Cube-FLAIR greatly improved CR. On the other hand, T1W-SE has better CR than BB Cube or BB Cube-FLAIR sequences in a range of relatively low Gd-DTPA concentrations less than 0.5 mmol/L

Table 5 Diagnosis of lesions, diagnostic basis, and observation period. This study was applied from June 2012 to December 2012. The observation period (from when the lesions were first pointed out until the last observation) was from September 2007 to August 2014

Patient number	Patient age/sex	Diagnosis	Diagnosis basis	Observation period (months)
1	64/M	Glioblastoma	Operation	46
2	68/M	Metastasis (Lung cancer)	Increased in size or number	27
3	53/M	Meningioma	Operation	82
4	67/M	Meningioma	Operation	33
5	57/F	Malignant lymphoma	Operation	21
6	80/M	Metastasis (Lung cancer)	Increased in size or number	15
7	30/M	Oligodendroglioma	Operation	26
8	58/F	Metastasis (Breast cancer)	Increased in size or number	14
9	70/F	Metastasis (Lung cancer)	Increased in size or number	8
10	41/M	Metastasis (Lung cancer)	Biopsy	30
11	56/F	Metastasis (Lung cancer)	Increased in size or number	11
12	54/F	Metastasis (Lung cancer)	Biopsy	39
13	64/M	Glioblastoma	Operation	26
14	62/F	Metastasis (Lung cancer)	Increased in size or number	23
15	64/F	Metastasis (Lung cancer)	Increased in size or number	22
16	82/F	Metastasis (Lung cancer)	Increased in size or number	6
17	70/M	Radiation necrosis	An enhanced lesion was increased about two years after RT, but there was no change one year later	51
18	60/F	Metastasis (Lung cancer)	Increased in size or number	28
19	73/F	Glioblastoma	Operation	23
20	52/F	Metastasis (Breast cancer)	Increased in size or number	79
21	85/M	Metastasis (Lung cancer)	FDG/PET showed accumulation in the right lung, ipsilateral pleura, and Th10 vertebral body	1
22	71/M	Metastasis (Lung cancer)	Increased in size or number	50
23	63/M	Hemangioblastoma	Operation	56

from CR measurement because the ROI could not be placed correctly. Each CR was calculated using the following equation: CR=(SI of lesion – SI of white matter) / SI of white matter. The mean values of the ROI (12.01 mm^2 on each side) were used to obtain signal-intensity measurements from the region of peak signal intensity corresponding to regions within the enhancing lesions and unaffected white matter in the contralateral hemisphere for the three sequences. The difference in CR between the sequences was analysed by single-factor analysis of variance (ANOVA).

Results

Phantom study

Images of the bottle phantom are shown in Fig. 1. The contrast shown by BB Cube was very similar to that of T1W-SE, while the contrast with BB Cube-FLAIR was different from that of T1W-SE and BB Cube. Based on this result, we decided to set repetition time (TR) of 500 ms and minimum TE (17.1 ms) for BB Cube in the clinical study by visual evaluation of Fig. 1a and b.

Figure 2 is a plot of the SI ratio between the sample tube phantom and normal white matter versus Gd concentration in the sample tube. BB Cube-FLAIR showed better CR than T1W-SE or BB Cube at a high Gd concentration. In addition, shortening of TR greatly improved CR in BB Cube-FLAIR. In contrast, T1W-SE showed better CR than BB Cube or BB Cube-FLAIR sequences at relatively low Gd-DTPA concentrations of less than 0.5 mmol/L. BB Cube-FLAIR with the shortest TR (600 ms) showed the best CR at all Gd concentrations among the three BB Cube-FLAIR sequences. From the results of this phantom study, we decided to set TR of 600 ms, inversion time (TI) of 300 ms, and minimum TE (17.9 ms) for BB Cube-FLAIR in the clinical study.

◀ **Fig. 3** (*a*) Contrast-enhanced T1W-SE image, (*b*) contrast-enhanced BB Cube image, and (*c*) contrast-enhanced BB Cube-FLAIR image from a 63-year-old patient with recurrence of hemangioblastoma. In all images, a neoplastic cyst with enhanced mural nodule in the right cerebellar hemisphere could be found. However, the enhanced small nodule (arrow) could be identified in BB Cube and BB Cube-FLAIR, but not in T1W-SE due to flow-related artefacts

Clinical study

Among the 44 subjects, 24 had identifiable lesions in the brain. One subject with metastasis derived from malignant melanoma was excluded from this study, as all lesions showed haemorrhage and were not suitable for evaluating the contrast enhancement effect. Thus a total of 23 subjects were ultimately evaluated for contrast enhancement effect. Ten cases were pathologically proven. Thirteen cases were diagnosed by previous and follow-up imaging. The diagnosis of lesions, diagnostic basis, and observation period in our patients are summarized in Table 5.

In terms of intracranial flow-related artefacts, the degree of flow-related artefacts was significantly lower for BB Cube and BB Cube-FLAIR than for T1W-SE ($p<0.01$). Effective suppression of flow-related artefacts in BB Cube sequences resulted in better conspicuity of lesions, especially in the posterior cranial fossa (Fig. 3). In addition, cortical veins were also effectively suppressed in BB Cube and BB Cube-FLAIR (Fig. 4).

In terms of detectability of the enhanced lesions, we were able to identify 182 lesions in 23 cases using T1W-SE, BB Cube, BB Cube-FLAIR, and coronal T1W-SE. A total of 63 lesions greater than 5 mm in diameter were detected with all sequences. Among 119 lesions less than 5 mm, 113 were metastases and 6 were recurrences of hemangioblastoma (Table 6). In six patients, eight small enhanced lesions that were well visualised on BB Cube and BB Cube-FLAIR images were not seen at all on T1W-SE images (Figs. 3, 5). In one patient with multiple metastases, two small enhanced metastases well visualised on T1W-SE and BB Cube images were not seen at all on BB Cube-FLAIR images (Figs. 4, 6). Detectability of lesions differed significantly among the three sequences (Cochran's Q test, $p=0.003$). There was a significant difference in detectability of lesions between T1W-SE and BB Cube (binomial test, $p=0.02$), but there were no significant differences in lesion detectability between T1W-SE and BB Cube-FLAIR or between BB Cube and BB Cube-FLAIR (binomial test $p=0.21$ and $p=0.15$, respectively). All interobserver and intraobserver agreements in lesion detectability were substantial (Table 7).

The mean CR on T1W-SE, BB Cube, and BB Cube-FLAIR were 0.61±0.37, 0.60±0.31, and 0.57±0.32, respectively. The CR of T1W-SE and BB Cube images were slightly

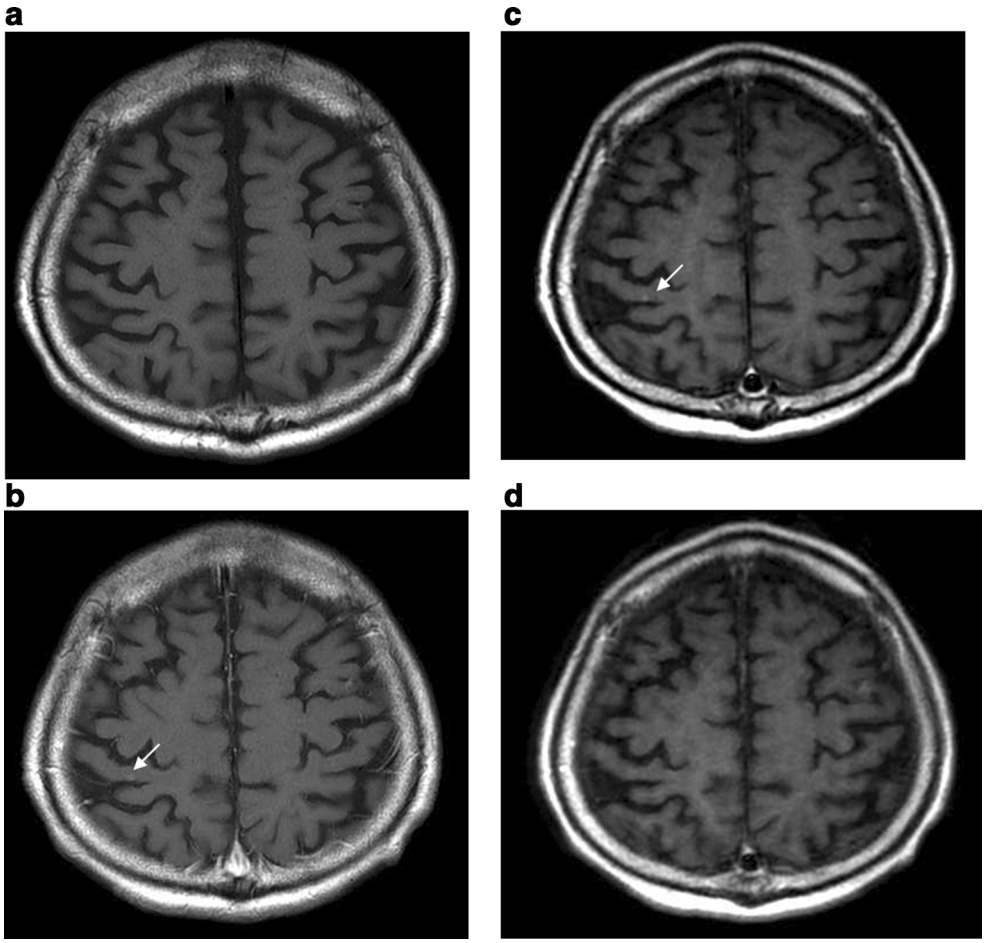

Fig. 4 (*a*) Pre-contrast T1W-SE image, (*b*) contrast-enhanced T1W-SE image, (*c*) contrast-enhanced BB Cube image, and (*d*) contrast-enhanced BB Cube-FLAIR image from a 68-year-old patient with multiple metastases from primary lung cancer. A small contrast-enhanced nodule in the right posterior central gyrus (*arrow*) was identified in T1W-SE and BB Cube, but not in BB Cube-FLAIR. In the T1W-SE image, a high signal of the cortical vein was observed, but the vein was well suppressed in BB Cube and BB Cube-FLAIR

higher than that of BB Cube-FLAIR, but with no significant difference (p=0.88).

Discussion

Flow-related artefacts are accentuated on T1W-SE images acquired after administration of Gd-DTPA as a result of the intraluminal T1-shortening effects of the contrast agent [8]. In contrast, in this study, there were no identifiable flow-related artefacts in any cases with BB Cube or BB Cube-FLAIR. In particular, the conspicuity of lesions in the posterior cranial fossa was better in BB Cube and BB Cube-FLAIR than in T1W-SE, and cortical veins were effectively suppressed in BB Cube and BB Cube-FLAIR. Cube sequence suppresses blood vessel signals, as blood flow causes phase dispersion with the use of low refocusing flip angles. For brain metastases, Komada et al. described the usefulness of contrast-enhanced SPACE (Sampling Perfection with Application optimized Contrasts by using different flip angle Evolutions), which is a sequence similar to Cube [9]. However, a fraction of the blood vessel signals

Table 6 Relationship between the size of lesions and lesion detectability

Sequence	Number of lesions detected (n=182 lesions)				Case
	Size of lesions<5 mm		Size of lesions 5 mm or more		
TIW-SE	111/119	(93 %)	63/63	(100 %)	17/23
BB Cube	119/119	(100 %)	63/63	(100 %)	23/23
BB Cube-FLAIR	117/119	(98 %)	63/63	(100 %)	22/23

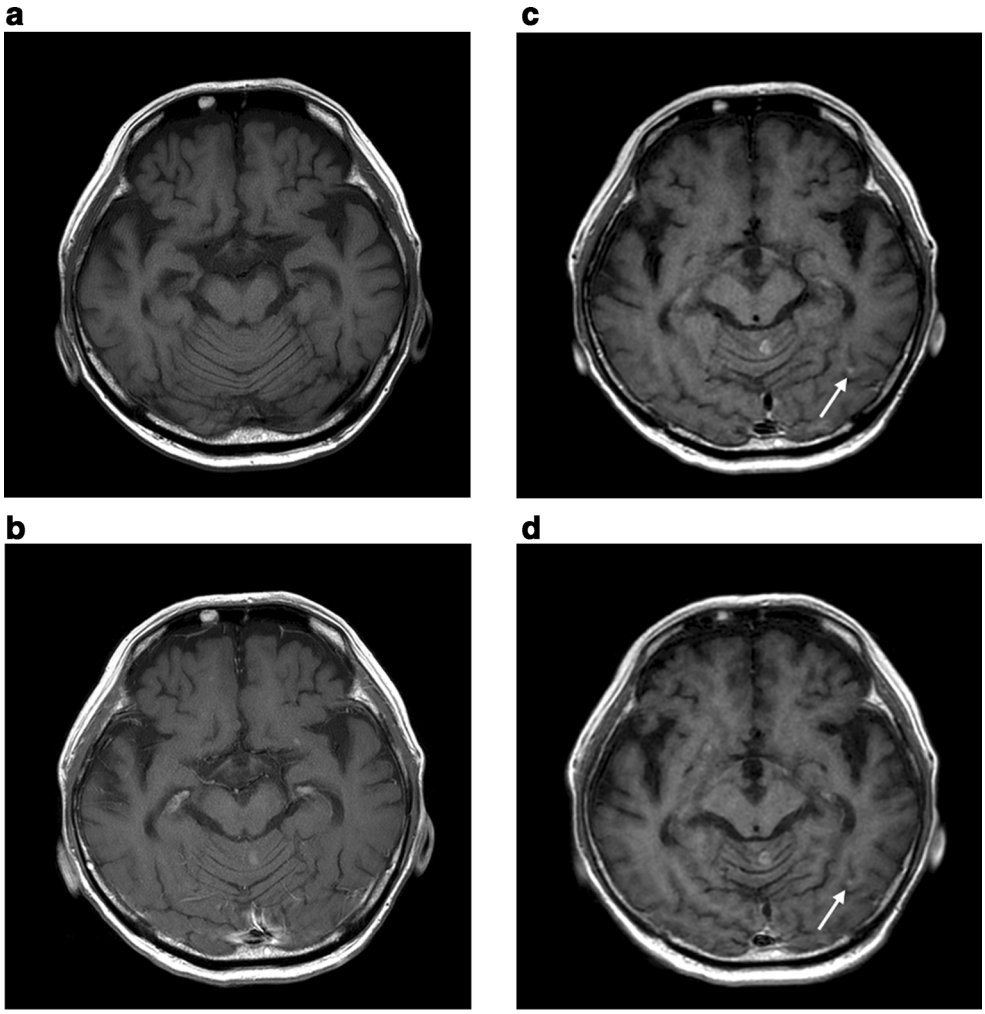

Fig. 5 (*a*) Pre-contrast T1W-SE image, (*b*) contrast-enhanced T1W-SE image, (*c*) contrast-enhanced BB Cube image, and (*d*) contrast-enhanced BB Cube-FLAIR image from a 68-year-old patient with multiple metastases from primary lung cancer. Several small enhanced lesions were detected. In T1W-SE, the small enhanced nodule in the left temporal lobe (*arrow*) could not be detected

remained visible in SPACE without the BB technique. Therefore, these suppression effects of arterial flow as well as cortical veins were useful for reading images to screen for small lesions and could be considered a strong advantage of this technique.

With regard to CR, there was no significant difference among T1W-SE, BB Cube, or BB Cube-FLAIR. Intracranial lesion contrast enhancement of 3D GRE sequences has been reported as less than that of conventional SE sequences at 1.5 T [1, 2]. Our equivalent CR suggests that BB Cube and BB Cube-FLAIR have the potential to show better conspicuity of lesions than 3D GRE when using a 1.5 T MR system.

In terms of the detectability of the enhanced lesions, BB Cube detected the highest number of lesions among the three pulse sequences. Furthermore, there was a significant difference in lesion detectability between T1W-SE and BB Cube. Because there was no significant difference in CR between sequences, the better detectability of BB Cube can be attributed to less partial volume effect as a result of thin-slice volume imaging and suppression of flow-related artefacts due to the BB technique. Thin-slice volume imaging of Cube would be useful for the detection of small lesions.

There was an interesting finding in some lesions, namely that contrast enhancement in BB Cube-FLAIR was clearly less than in BB Cube and T1W-SE. Although we did not determine the reason for this, the fact that T1 contrast in BB Cube-FLAIR was superior to that in BB Cube suggests that such lesions might show a low signal compared to the surrounding white matter on pre-contrast BB Cube-FLAIR images. BB Cube-FLAIR actually showed better contrast of infarction in the splenium of the corpus callosum than BB Cube or T1W-SE (Fig. 7). Therefore, the contrast enhancement produces isointensity of the lesions only in relation to the white matter. This phenomenon is similar to that seen in metastases within fatty bone marrow on contrast-enhanced T1W-SE images. In addition, the BB Cube-FLAIR sequence had the

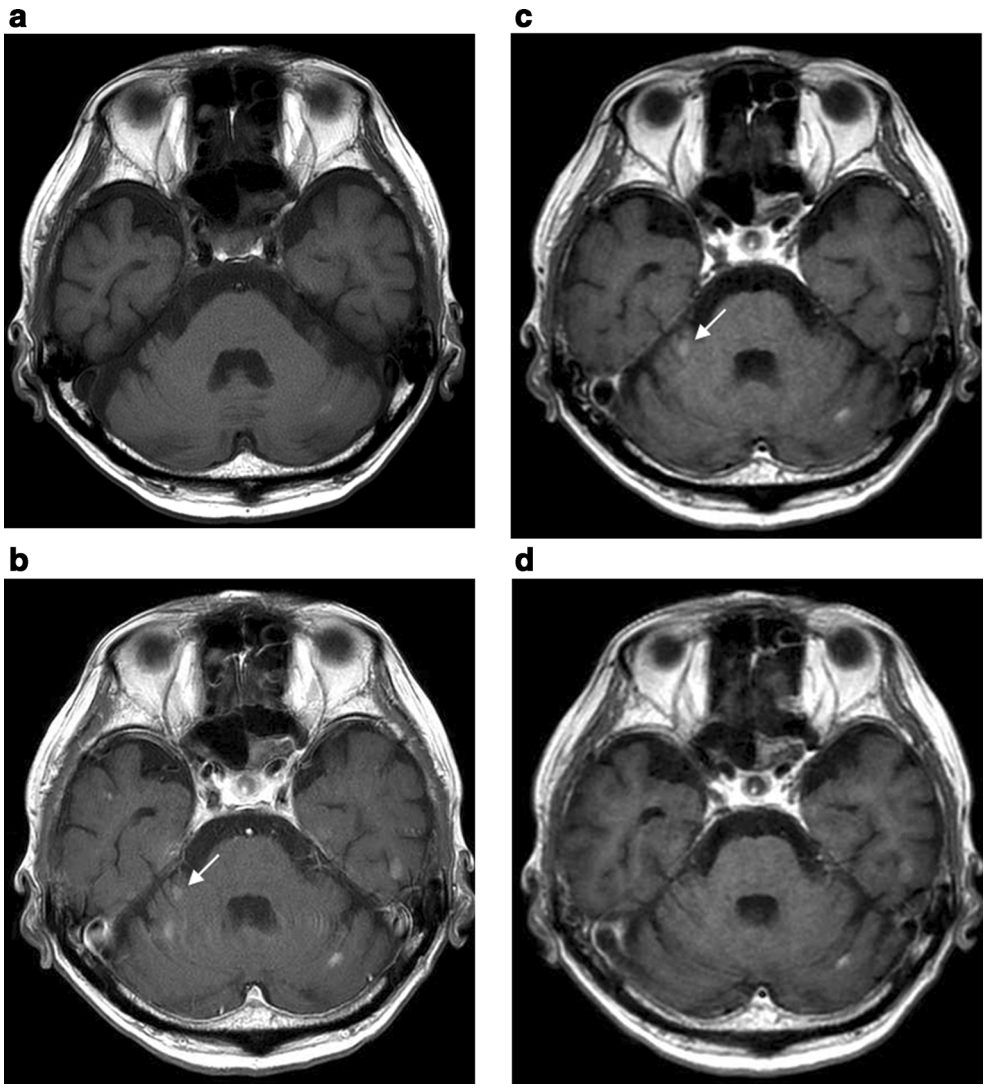

Fig. 6 (*a*) Pre-contrast T1W-SE image, (*b*) contrast-enhanced T1W-SE image, (*c*) contrast-enhanced BB Cube image, and (*d*) contrast-enhanced BB Cube-FLAIR image from the same case as in Fig. 4. Highly enhanced lesions were observed. The lesion indicated by an *arrow* was visible in T1W-SE and BB Cube, but not in BB Cube-FLAIR

worst CR among the three sequences in a range of relatively low Gd-DTPA concentrations (less than 0.5 mmol/L) in our second phantom study. Hence, we consider there to be no significant difference in lesion detectability between T1W-SE and BB Cube-FLAIR, even though the latter is accompanied by thin slice thickness and the BB imaging technique. Unfortunately, our study was designed to evaluate only contrast-enhanced BB Cube and BB Cube-FLAIR images.

Table 7 The degrees of interobserver and intraobserver agreement in detectability of lesions

	Interobserver agreement Kappa	Intraobserver agreement Kappa
T1W-SE (n=174)	0.62	0.78
BB Cube (n=182)	0.65	0.76
BB Cube-FLAIR (n=180)	0.65	0.74

Some investigations using a 3 T MR unit have demonstrated that 3D GRE shows the best detectability of intracranial lesions compared to 2D SE and IR SE as a result of thin-slice acquisition, even though the CNR of 3D GRE is less than those of 2D SE and IR SE [10]. On the other hand, at 1.5 T, the lesion contrast enhancement of 3D GRE has been reported to be less than that of 2D SE, and there was a risk of missing the lesions in 3D GRE [1, 2]. BB Cube and BB Cube-FLAIR, however, have equivalent contrast to that of 2D SE and allow thin-slice volume acquisition, suggesting that BB Cube is a promising technique for the detection of small brain lesions.

On the other hand, the results of our second phantom study showed that the CR of T1W-SE was better than that of BB Cube or BB Cube-FLAIR sequences in a range of relatively

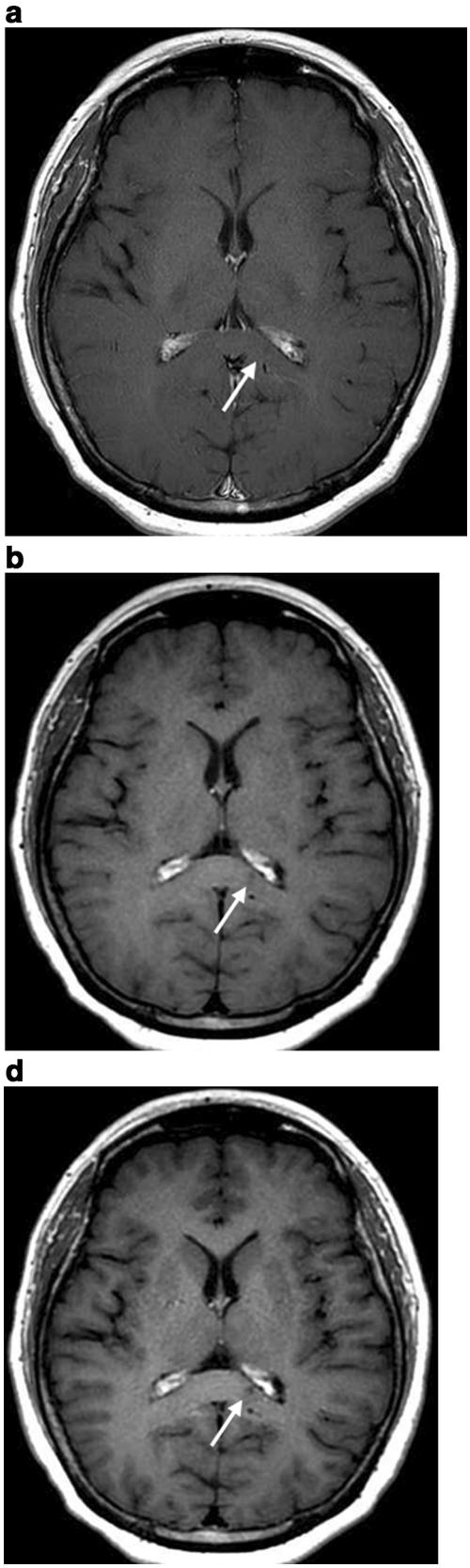

◀ **Fig. 7** (*a*) Contrast-enhanced T1W-SE image, (*b*) contrast-enhanced BB Cube image, and (*c*) contrast-enhanced BB Cube-FLAIR image from a 50-year-old patient with cerebral infarction. There was a small area showing unenhanced low signal on the left side of the splenium of the corpus callosum. The negative contrast of the area was better in BB Cube-FLAIR than in BB Cube or T1W-SE

low Gd-DTPA concentrations. Since T1W-SE may show better contrast than BB Cube and BB Cube-FLAIR in this concentration range, there is a risk of missing some lesions associated with a low concentration of Gd-DTPA. We recommend the addition of T1W-SE to BB Cube acquisition in order to avoid missing such lesions.

We employed lesion CR in this study, as calculation of the signal-to-noise ratio and contrast-to-noise ratio cannot be accurately performed on only one image set when parallel imaging is used; the subtraction method is the preferred technique to evaluate these parameters for scans performed with parallel imaging [11], since two consecutive scans with three different image sequences would not be ethically justified in the patient group.

There are some limitations in this study. First, the three sequences were started at different times after the injection of contrast agent. However, Yuh et al. found no significant difference in the number of lesions detected with a delay of 10 min between injection of contrast and imaging [12]. In our cases, the scans were completed within 13 min. Therefore, we think that the delayed enhancement effect in our study is so small as to be negligible. Second, we could not obtain histological confirmation of the diagnosis in several subjects. Although some false-positive lesions may have been included in our subjects, we believe that our careful observation, including interpretation of previous and/or follow-up imaging studies, minimized the possibility of false positives. Third, in the clinical study, there was a significant difference in CR among the three sequences. The lesions used for CR measurement were relatively large and tended to show sufficient uptake of Gd-DTPA. However, the lesions that showed different conspicuity among the sequences were small and had weak enhancement of Gd-DTPA. Our CR measurement did not include such small and weakly enhanced lesions, which may explain why there was no significant difference in CR among the sequences.

Conclusions

BB Cube had lesion contrast enhancement equivalent to that of 2D SE, allowed thin-slice volume acquisition without flow-

related artefacts, and demonstrated the best detectability of intracranial lesions among the three pulse sequences. We can conclude that BB Cube is a promising screening technique for the detection of small intracranial lesions at 1.5 T MRI.

Acknowledgments The scientific guarantor of this publication is Professor Takamichi Murakami, Department of Radiology, Kinki University Faculty of Medicine. The authors of this manuscript declare no relationships with any companies whose products or services may be related to the subject matter of the article. The authors state that this work has not received any funding. One of the authors has significant statistical expertise. Institutional review board approval was obtained. Written informed consent was obtained from all subjects (patients) in this study. No study subjects or cohorts have been previously reported. Methodology: prospective, diagnostic or prognostic study, performed at one institution.

References

1. Chappell PM, Pelc NJ, Foo TK et al (1994) Comparison of lesion enhancement on spin-echo and gradient-echo images. AJNR Am J Neuroradiol 15:37–44
2. Brant-Zawadzki M, Gillan GD, Nitz WR (1992) MP RAGE: a three-dimensional, T1-weighted, gradient-echo sequence initial experience in the brain. Radiology 182:769–775
3. Mugler JP III (2014) Optimized three-dimensional fast-spin-echo MRI. J Magn Reson Imaging 39:745–767
4. Park J, Kim EY (2010) Contrast-enhanced, three-dimensional, whole-brain, black-blood imaging: application to small brain metastases. Magn Reson Med 63:553–561
5. Naganawa S, Satake H, Iwano S et al (2008) Contrast-enhanced MR imaging of the brain using T1-weighted FLAIR with BLADE compared with a conventional spin-echo sequence. Eur Radiol 18: 337–342
6. Melhem ER, Bert RJ, Walker RE (1998) Usefulness of optimized Gadolinium-enhanced fast fluid-attenuated inversion recovery MR imaging in revealing lesions of the brain. AJR Am J Roentgenol 171:803–807
7. Landis JR, Koch GG (1977) The measurement of observer agreement for categorical data. Biometrics 33:159–174
8. Richardson DN, Elster AD, Williams DW III (1990) Gd-DTPA-enhanced MR images: accentuation of vascular pulsation artifacts and correction by using gradient-moment nulling (MAST). AJNR Am J Neuroradiol 11:209–210
9. Komada T, Naganawa S, Ogawa H et al (2008) Contrast-enhanced MR imaging of metastatic brain tumor at 3Tesla: utility of T1-weighted SPACE compared with 2D spin echo and 3D gradient echo sequence. Magn Reson Med Sci 7:13–21
10. Kakeda S, Korogi Y, Hiai Y et al (2007) Detection of brain metastasis at 3 T: comparison among SE, IR-FSE and 3D-GRE sequences. Eur Radiol 17:2345–2351
11. Goerner FL, Clarke GD (2011) Measuring signal-to-noise ratio in parallel imaging MRI. Med Phys 38:5049–5057
12. Yuh WTC, Tali ET, Nguyen HD et al (1995) The effect of contrast dose, Imaging time, and lesion size in the MR detection of intracerebral metastasis. AJNR Am J Neroradiol 16:373–380